JOURNAL OF CATALYSIS 78, 380–388 (1982)

Electron Spin Resonance of Supported and Unsupported Molybdenum Hydrotreating Catalysts

I. Model System Studies

B. G. SILBERNAGEL, T. A. PECORARO,[1] AND R. R. CHIANELLI[2]

Corporate Research—Science Laboratories, Exxon Research and Engineering Company, Linden, New Jersey 07036

Received February 8, 1982; revised June 29, 1982

A combination of different synthetic techniques, dibenzothiophene desulfurization activity studies, and electron spin resonance observations are used to explore the relation between defects and hydrodesulfurization (HDS) activity for bulk molybdenum sulfides and supported, sulfided Mo/γ-Al_2O_3 catalysts. A linear correlation is found between sulfur-coordinated Mo^{5+} defects and HDS activity for both unsupported and supported samples. Comparison with oxygen chemisorption and magnetic susceptibility data suggests that these defects are associated with a fraction of the edge sites of molybdenum sulfide crystallites.

I. INTRODUCTION

We have used the technique of electron spin resonance (ESR) to characterize magnetic defects in unsupported and supported molybdenum oxides and sulfides. The goal of this effort is to trace changes in the morphology of these molybdenum defect species and their influence on catalytic hydrotreating processes. The present report illustrates the techniques, providing selected examples of the range of its potential application. We find that ESR observations of these materials yield defect densities which correlate with activity for the catalytic hydrodesulfurization of dibenzothiophene (DBT). Further, the position and shape of the ESR absorption provide specific information about the chemistry of these molybdenum species, the form of their ligands, and the symmetry of their local environments.

ESR is a tool of great potential utility in catalyst studies. It is a highly sensitive probe of defect sites in a material: unpaired electron spins and "dangling bonds" which are likely to be chemically active. Such defects are quite routinely observed at the parts per million level with ESR. In complex systems, like supported transition metal catalysts, there are likely to be several paramagnetic components and it is important to identify the various different species. For a typical commercial catalyst like Co–Mo/γ-Al_2O_3, one might expect to observe ESR absorptions from paramagnetic cobalts and molybdenum species (most likely Co^{2+} and Mo^{5+}, Mo^{3+}) as well as an assortment of radical forms which appear on the catalyst during the sulfidation process or DBT activity tests. These include carbon radicals: C^0, SO_2^-, O_2^-, O^-, which have all been reported previously. A brief summary of the strategy applying ESR to such catalysts (*1*) and a detailed analysis of supported molybdena–alumina catalysts (*2*) have appeared recently.

In principle, an analysis of the position, width, and shape of other ESR absorptions can identify the type of defect and provide

[1] Current address: Chevron Research Company, 576 Standard Avenue, Richmond, Calif. 94804.

[2] Author to whom correspondence should be addressed.

0021-9517/82/120380-09$02.00/0

specific information about the defect site, including the *valence* of the defect species (particularly for *d* electron transition metals), the *type of atoms adjacent to the defect site*, the *site symmetry*, and the *number* of the sites. With sufficient care the site density can be determined with an accuracy of approximately ±5–10%. Because of the strong interaction between the electron spin and its environment, it is difficult to calculate the ESR properties of a particular transition metal defect ab initio. However, by examining carefully synthesized and well-documented model systems it is possible to identify different defect sites by their characteristic "signatures." A major issue is whether these defects, which can be extremely small in number, reflect either the bulk properties of the material and/or their catalytic properties. For molybdenum sulfides, this appears to be the case: a defect density/DBT activity correlation exists and the defect density appears to reflect the morphology of the molybdenum sulfide crystallites. In the following sections, we will present data on a series of carefully prepared model systems and compare the results with other examples of recent research on related materials (*2–5*).

II. EXPERIMENTAL DATA UNSUPPORTED MOLYBDENUM SULFIDES

The key to understanding such complicated catalysts is to begin with an analysis of significantly simpler model systems, the unsupported molybdenum sulfides. They are important, since molybdenum is clearly an active component in the Co–Mo catalyst. They are much simpler samples to study since there are no support or transition metal promoter effects. Furthermore, bulk MoS_2 has no intrinsic ESR absorption so that the defect signals appear without any complicated background. This is an important consideration since defect densities are relatively low—typically on the order of 1 in 10^3 to 1 in 10^5 of the Mo atoms present. Different preparation techniques produce broad variations in surface area of the resulting sulfides (typically from 1 to 200 m^2/g), as well as in their morphology (*6*). As expected, there are also dramatic variations in their catalytic activity—particularly as examined by the desulfurization of dibenzothiophene (DBT).

In general, sulfides have a number of defect sites observable by ESR. An example of this is shown in Fig. 1, an ESR spectrum of MoS_3 obtained from the decomposition of $(NH_4)_2MoS_4$ at 150°C in a vacuum furnace. Three traces appear in the figure. The bottom trace is the integrated ESR absorption spectrum, proportional to the number of paramagnetic species at a given field value for measurements made at a constant frequency (in this case 35.010 GHz). The top trace is the derivative of the absorption, which is particularly useful since the derivative curve exhibits a high level of articulation, indicating the presence of several inequivalent molybdenum defect types, with absorptions occurring at different values of the magnetic field. To understand the source of the individual components, we have synthesized a series of model systems, employing techniques which produce materials with reproducible types and members of defects. On this basis, the complex spectrum in Fig. 1 can be analyzed with some confidence.

One model system chosen for study was the organometallic complex molybdenum trisdithiolene, which can be quantitatively reduced by reaction with $NaBH_4$ in diglyme (*7*). The resulting molybdenum species is formally pentavalent and coordinated with six sulfur atoms in a configuration similar to that encountered in MoS_2. The resulting solution ESR signal (Fig. 2A) provides a measure of the isotropic g value which might be anticipated for sulfur-coordinated, thio-Mo^{5+}, species. A symmetric, narrow (splitting between derivative maxima, $\Delta H_{pp} \sim 7$) signal is observed with $g = 2.0091$, in good agreement with previous reports (*8*).

Although many molybdenum sulfides yield a complex spectrum of the type shown in Fig. 1, we find that sulfides with

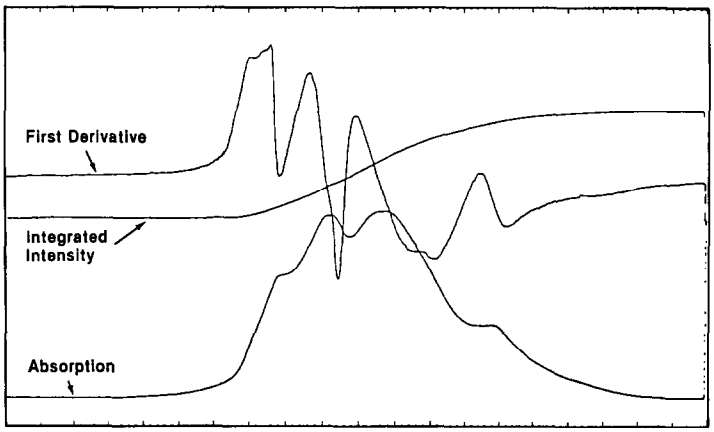

FIG. 1. A nominal "MoS_3" sample shows several defect sites. Appropriate resonance parameters: Microwave frequency, 35.010 GHz; scan range, 2 kG; magnetic field center, 12,505.0 G; modulation amplitude, 4 G.

the approximate stoichiometry MoS_2, when subjected to conditions similar to those encountered in hydrotreating, almost invariably exhibit a thio-Mo^{5+} signal of the type shown in Fig. 2B. The MoS_2 material whose spectrum is shown in Fig. 2B was formed by precipitation from a $MoCl_4$ and Li_2S reaction in an ethyl acetate solution and then sulfided in a 15 wt% H_2S/H_2 gas mixture at 350°C for 1 hr (*6*). The resulting ESR absorption consists of a narrow signal with $g = 2.004$ superimposed on a broader (~120 G) spectrum. Since these samples were sulfided and sealed without exposure to air, we propose that the narrow absorption is associated with a sulfur radical species (*5*). Subsequent DBT desulfurization tests diminish or eliminate this narrow absorption (*9*). The underlying broad absorption is not changed in intensity by the desulfurization tests. The broad component is asymmetric and typical of an axially symmetric g-value tensor, with $g_{\|} = 2.0380$ and $g_{\perp} = 2.0038$. The mean g value, obtained by finding the center of gravity of the absorption, is 2.0096, quite similar to that seen for Mo-trisdithiolene.

Samples with compositions approximately MoS_3 are readily obtained by thermal decomposition of $(NH_4)_2MoS_4$ at temperatures of 300°C (*9, 10*). The ESR absorption (Fig. 2C) is significantly different from that of the MoS_2 case. The line is broader (~150 G), and the derivative signal is significantly different. The narrow component seen for MoS_3 is broader and does not exhibit a symmetric derivative. While it is not possible to specify a resonance center for this narrow component its approximate position is similar to that of the narrow component in MoS_2. This ESR "signature" is reproducibly obtained and similar in general form to the absorption for MoS_3 recently reported by Basetto *et al.* (*5*). The absorption lineshape has an obviously lower symmetry than that for the MoS_2 case. Assuming a single paramagnetic species and a nonaxial g-value tensor, values of $g_1 = 2.0492$, $g_2 = 2.0180$, and $g_3 = 1.9736$ are obtained from analysis of inflection points of the derivative spectrum and spectrum simulation. In spite of these apparent differences, the mean g value, 2.0162, is similar to that of the other thio-Mo^{5+} defects.

As an example of an oxygen-coordinated defect, we chose to examine samples of MoO_3 which had been reduced by refluxing in tetrahydroquinoline at temperatures of 250°C, for 8 hr. The resulting oxo-Mo^{5+} defect is shown in Fig. 3. It is described by an axially symmetric g tensor with $g_{\perp} = 1.932$

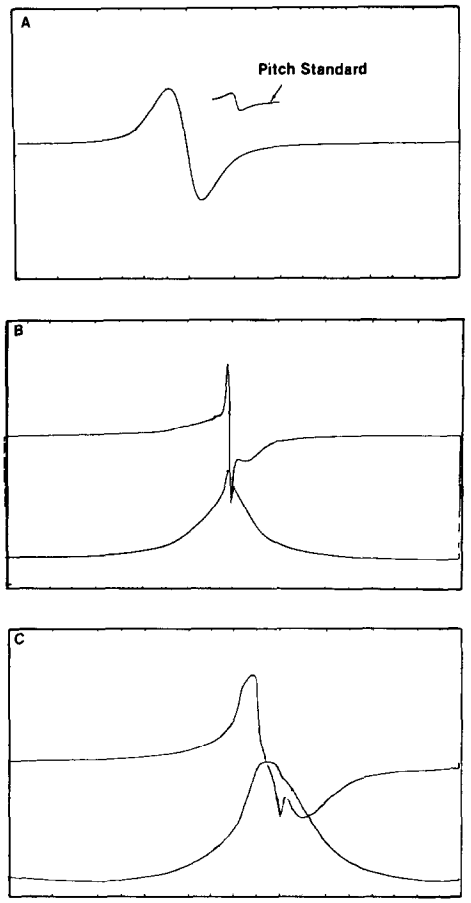

FIG. 2. Model molybdenum sulfide systems. (A) Mo-trisdithiolene reduced by $NaBH_4$ in diglyme. Frequency, 9.0784 GHz; scan range, 100 G; magnetic field center, 3242.0 G; modulation, 0.5 G. (B) MoS_2—Frequency, 9.0782 GHz; scan range, 1 kG; magnetic field center, 3242.0 G; modulation, 5 G. (C) MoS_3—Frequency, 9.5068 GHz; scan range, 1 kG; magnetic field center, 3250 G; modulation, 5 G.

and $g_{\|} = 1.885$. These values are in good agreement with the body of literature on Mo^{5+} defects in oxides (*2*). The model system ESR data are enumerated in Table 1.

The ESR intensities for these MoS_2 and MoS_3 defects have been determined with respect to a Varian weak-pitch carbon standard and are presented for a series of sulfide samples in Table 2. The intensities, approximately 10^{18} spins/g sample, correspond to $\sim 2 \times 10^{-4}$ spins/atom of molybdenum. These ESR intensities are compared with BET surface areas, oxygen chemisorption levels, and the catalytic activity level for the desulfurization of dibenzothiophene in an autoclave reaction (*9*). Figure 4A shows the almost linear variation of ESR intensity with DBT activity which suggests a connection between the molybdenum defects and the catalytic process. A similar linear variation is seen for the level of oxygen chemisorbed (Fig. 4B) (*9*). By contrast, the correlation between BET surface area and hydrodesulfurization (HDS) activity is weak (Fig. 4C). This suggests that not only the MoS_2 surface area but also the types of surfaces are significant (*6*). The surfaces most likely to absorb oxygen and to contain paramagnetic molybdenum atoms are the defects (edges, corners, etc.) in the layered MoS_2 structure.

While both ESR and O_2 chemisorption reflect the HDS activity of these catalysts, a simple estimate of the magnitudes of these two effects suggests that they are not necessarily associated with the same site. Taking the first sample of Table 2 as an example, 31 μmole of O_2 chemisorbed per gram of the final MoS_2 product implies that there are 9.9×10^{-3} oxygen atoms absorbed per molybdenum atom. Conversely, 2.3×10^{18} thio-Mo^{5+} spins/g sample implies 6.1×10^{-4} paramagnetic molybdenum species observed per molybdenum. This 15-fold difference in the number of sites observed can be explained by attributing oxygen chemisorption to all edge sites on the MoS_2 crystallites and asserting that only a subset of these edge sites, perhaps corner sites, are seen in ESR. Studies on the reduction of MoO_3 on γ-Al_2O_3 (*2, 11*) provide parallel evidence. These oxide studies (*2*) and recent magnetic susceptibility measurements on MoS_3 materials (*12*) suggest that all the edge sites are, in fact, paramagnetic but unobservable because of exchange interactions between neighboring sites.

Supported MoO_3/γ-Al_2O_3 Catalysts

Supported MoO_3/γ-Al_2O_3 catalysts with various Mo loadings were presulfided at

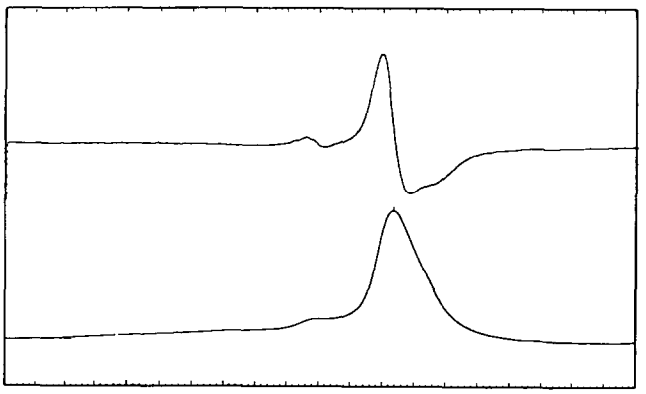

FIG. 3. A model oxide defect: MoO_3 refluxed in tetrahydroquinoline. Frequency, 9.0757 GHz; scan range, 1 kG; magnetic field center, 3252.0 G; modulation, 5 G.

TABLE 1

ESR Parameters for Model Systems

	Derivative analysis		Computer analyses	
			g_{mean}	$\Delta H_{1/2}$[a] (G)
Mo-trisdithiolene (reduced in diglyme)	$\langle g \rangle = 2.0091$	$\Delta H_{pp} = 7.0$ G		
MoS_2 (sulfided at 350°C)	$g_{\parallel} = 2.0380$	$g_{\perp} = 2.0038$	2.0096	119.5
MoS_3 ($(NH_4)_2MoS_4$ decomposition)	$g_1 = 2.0492$ $g_2 = 2.0180$	$g_3 = 1.9736$	2.0162	153.8
MoO_3 (THQ reduced)	$g_{\parallel} = 1.8848$	$g_{\perp} = 1.9322$		
MoO_3 (H_2/H_2S reduced)				
Oxo	$g_{\parallel} = 1.8849$	$g_{\perp} = 1.9342$		
Thio	$g_{\parallel} = 2.0287$	$g_{\perp} = 1.9975$		

[a] Measured at 9.5 GHz.

TABLE 2

Characterization and Catalytic Data for Bulk Molybdenum Sulfide Catalysts[a]

Starting material	Activity (μmole DBT/g-sec)	BET surface area (m^2/g)	O_2 chemisorption (μmole/g)	ESR intensity ($\times 10^{18}$ spins/g)
MoS_3	0.37	114	31	2.30
MoS_3	0.33	120	35	1.85
MoS_3	0.27	88	27	1.23
MoS_3	0.18	112	19	0.83
MoS_2	0.18	35	—	0.74
MoS_2	0.15	27	11	0.51
MoS_2	0.13	43	—	0.84

[a] MoS_3 samples were prepared by methods described in Refs. (*9*, *10*). MoS_2 samples were prepared by methods described in Ref. (*6*).

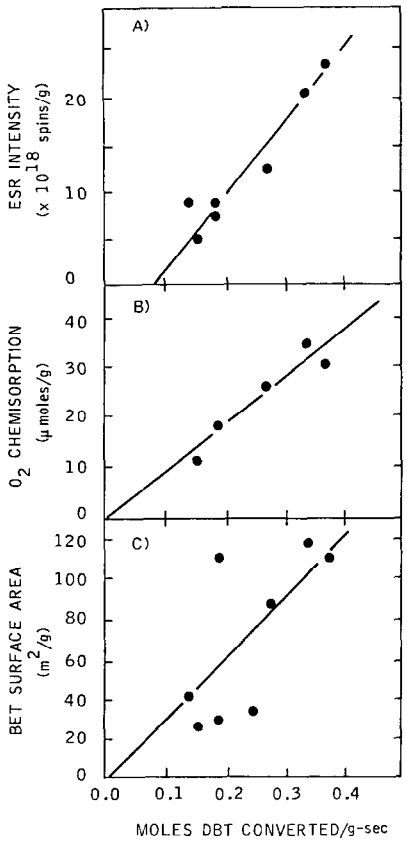

FIGURE 4

350°C for 45 min with a 15 wt% H_2S/H_2 mixture and then subjected to DBT tests. The calcined catalysts show no Mo ESR signals prior to sulfidation, confirming the presence of the Mo^{6+} state. Two ESR signals appear upon sulfidation, as shown in Fig. 5. The conspicuous signal observed at higher field (on the right-hand side of the figure) has a *g* value of 1.931, appropriate for an oxo-Mo^{5+} species. The well-articulated asymmetry observed in tetrahydroquinoline (THO)-reduced MoO_3 (Fig. 3), does not appear here, suggesting that there may be some distribution in site types. A second, lower-field absorption corresponds very closely to the thio-Mo^{5+} defect in MoS_2, shown in Fig. 2B.

This H_2S/H_2 reduction process can be modeled by examining the direct reduction of MoO_3 under similar conditions, as shown in Fig. 6 (*13*). The oxo-Mo^{5+} signal appropriate to reduced MoO_3 (Fig. 7) and the thio-Mo^{5+} signal appropriate to MoS_2 (Fig. 2A) are both observed. The high degree of articulation of the derivative signal suggests that the two site types are unique in this case. The approximate paramagnetic density is 5.2×10^{-4} spins/molybdenum atom, comparable to the values observed for the sulfides.

Detailed ESR and chemisorption data for the supported sulfides are presented in Fig. 7 and Table 3. The figure shows a nearly linear increase in oxygen chemisorption and thio-Mo^{5+} defect density levels with molybdenum loading. By contrast oxo-Mo^{5+} defect levels are nearly constant. This suggests that some fraction of the molybdenum oxide deposited on the catalyst support is stabilized by interactions with the surface, either by epitaxial effects or selective interaction with support surface defects. A similar preferential generation at stable sites occurs during VO^{2+} deposition on alumina catalyst supports in the early phases of residfining runs (*14*).

A comparison of O_2 chemisorption levels and ESR spin densities reveals the much greater metals dispersion on the catalyst support. For the 4.07 wt% Mo-loaded sample, for example, the 54 μmol/g of adsorbed O_2 corresponds to 0.25 O atoms adsorbed/Mo atom, a 25-fold increase over the unsupported case. The ESR spin densities for

TABLE 3

Characterization Data for Sulfided MoO_3/γ-Al_2O_3[a]

Mo loading (wt%)	O_2 chemisorption (μmole/g)	ESR intensity (×10¹⁸ spins/g)	
		Oxo-Mo^{5+}	Thio-Mo^{5+}
4.07	54	4.60	3.31
7.22	74	5.39	4.76
10.3	111	6.48	6.41

[a] Catalysts were prepared by incipient wetness impregnation of $(NH_4)_2Mo_7O_{14}$ on Al_2O_3 followed by calcining in air at 500°C, and then sulfiding in H_2/15% H_2S at 350°C for 1 hr.

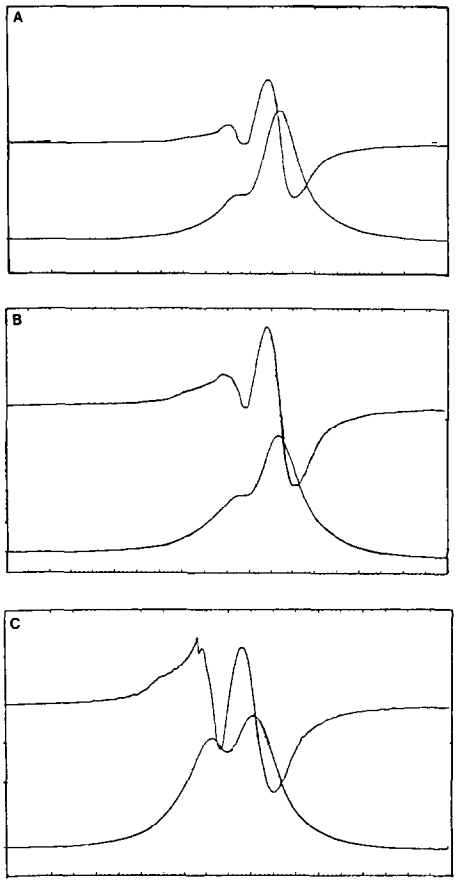

FIG. 5. Sulfided MoO_3/γ-Al_2O_3 catalysts with various molybdenum loadings. (A) 4.07 wt% Mo. Frequency, 9.0873 GHz; scan range, 1 kG; magnetic field center, 3242 G; modulation, 5 G. (B) 7.22 wt% Mo. Frequency, 9.5035 GHz; scan range, 1 kG; magnetic field center, 3390 G; modulation, 5 G. (C) 10.3 wt% Mo. Frequency, 9.5040 GHz; scan range, 1 kG; magnetic field center, 3390 G; modulation amplitude, 5 G.

these samples correspond to 0.018 oxo-Mo^{5+} defects/Mo atom and 0.013 thio-Mo^{5+} defects/Mo atom, also 25-fold enhancements. In the ratio of oxygen chemisorbed to Mo^{5+} ESR density remains ~10–20, as in the unsupported case. The correlation of these intensities with DBT activity is quite complex and will be discussed elsewhere.

III. DISCUSSION

The goal of the present paper has been to document certain classes of molybdenum atom defect sites in well-defined sulfide and oxide model systems, to establish their relationship to catalytic desulfurization, and to demonstrate their occurrence on conventional catalyst supports. While there are undoubtedly many paramagnetic species that can occur on catalysts (*3*, *4*), present experiments suggest that, under typical HDS conditions, there are two major molybdenum species which are observable, which we have called oxo-Mo^{5+} and thio-Mo^{5+}. While other species, like MoS_3, do occur at lower temperatures, they do not survive for extended periods at 350°C. A similar thio-Mo^{5+} signal occurs for molybdenum sulfides produced in a variety of ways, with surface areas which vary from 1 to 150 m^2/g. The defect density measured by ESR correlates with the rate of DBT desulfurization and the amount of O_2 which can be chemisorbed. The significant difference between chemisorption levels and spin densities suggests that an ESR signal is observed from only a fraction of the total number of edge sites on the MoS_2 crystallites. While supported MoS_2 has a 25-fold increase in edge sites over the unsupported samples, the relative numbers of oxygen atoms adsorbed and paramagnetic species remain constant, suggesting a similar molybdenum sulfide morphology.

The present data clarify the character of the defect sites. In principle, knowledge of the ion valence, ligand type, and site symmetry is sufficient for an ab initio calculation of the ESR properties. The situation is seldom so simple in practice. ESR properties depend sensitively on the character of the metal ion, particularly in cases like the present one in which the bonds have a significant amount of covalent character. Inferences about the chemical form and site character of the defect are usually based on arguments which combine chemical information, knowledge of the atomic structure of the materials, and the ESR properties. An example of this line of reasoning is the assignment of the ESR absorptions for thermal decomposition products of $(NH_4)_2WS_4$ (*15*), in which the defects in high-tempera-

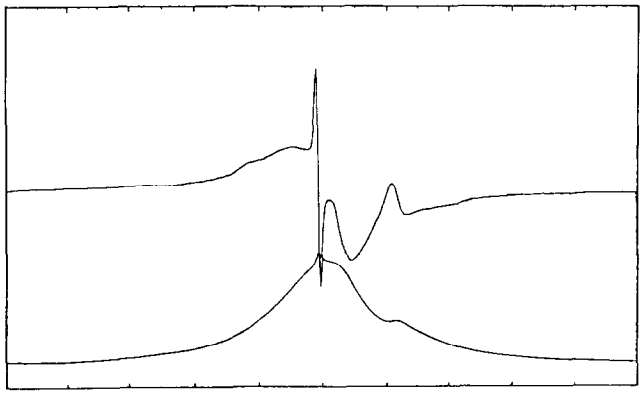

FIG. 6. MoO_3 reacted with H_2/H_2S shows both oxide and sulfide defects. Frequency, 9.5013 GHz; scan range, 1 kG; magnetic field center, 3400 G; modulation, 5 G.

ture decomposition products were attributed to a W^{3+} species. Similar statements have been made about the defects in reduced molybdenum oxides. However, it is important to note that the site symmetry cannot necessarily be uniquely determined from ESR parameters such as the g value (*16*). Recent systematic studies of reduced molybdena–alumina catalysts, employing 9.5- and 35-GHz ESR measurements, temperature variations from 4.2 to 1200 K, and site titrations with various molecular species, suggest that the reduced molybdenum species occur as oxo-Mo^{5+} forms present in tetrahedral sites on the surface of the alumina (*2*).

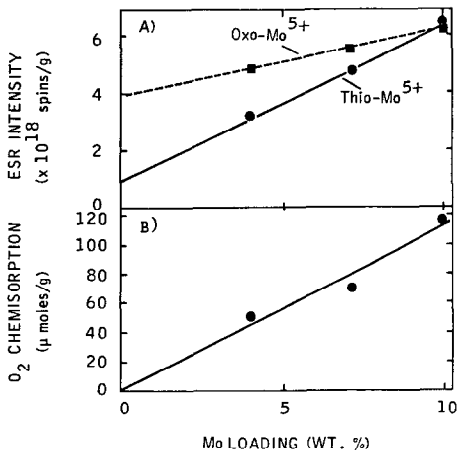

FIGURE 7

For the present molybdenum sulfide model systems, many of the same techniques have been employed including 9- and 35-GHz analyses and temperature dependence studies from 5 to 500 K. As in the oxide case, the fact that the g values are frequency independent and the fact that the ESR absorption does not change in character at temperatures as low as 5 K suggest that the molybdenum defects occur with a nominal Mo^{5+} valence. By contrast, Mo^{3+} species in low-symmetry crystalline field environments would be expected to have highly anisotropic g values and a finite crystal field splitting term, producing frequency-dependent changes in the position and shape of the ESR absorption (*17*). Mo^{3+} species in high-symmetry sites would have rapid spin lattice relaxation rates and exhibit significant variations in lineshape with temperature. Conversely, Mo^{5+} species have frequently been observed, with g values in the range of 1.90–2.01 (*18*).

The g-value magnitudes are still the subject of calculation. As in the Mo^{5+}-tris-dithiolene case, a g value of ~2.01 is consistent with the electronic properties of the system (*8*). It is interesting that, while there are large differences in g values for oxo-Mo^{5+} and oxo-W^{5+} defects, ~1.93 and ~1.57 (*19*), respectively, the corresponding thio g values are ~2.01 and ~2.03 (*15*). This similarity in g value may be associated

with a greater delocalization of the d' electron on the metal atom. A detailed analysis of the g values of model sulfide systems will appear elsewhere.

ACKNOWLEDGMENTS

We gratefully acknowledge T. R. Halbert, A. J. Jacobson, F. J. Parker, and A. F. Ruppert for assistance in various aspects of the sample preparation. L. A. Gebhard collected the ESR data and S. J. Tauster provided the chemisorption results prior to their separate publication (*9*). We thank E. I. Stiefel for several interesting discussions.

REFERENCES

1. Silbernagel, B. G., *in* "Nuclear and Electron Resonance Spectroscopies Applied to Materials Science" (E. I. Kaufmann and G. Shenoy, Eds.), p. 117. Elsevier/North-Holland, Amsterdam, 1981.
2. Abdo, S., "Investigation of Molybdenum-Alumina Catalysts by Electron Paramagnetic Resonance." Thesis, University of Wisconsin, Milwaukee, 1981.
3. Konings, A. J. A., van Dooren, A. M., Koningsberger, D. C., de Beer, J. H. J., Farragher, A. L., and Schuit, G. C. A., *J. Catal.* **54,** 1 (1978).
4. Konings, A. J. A., Brentjens, W. L. J., Koningsberger, D. C., and de Beer, V. H. J., *J. Catal.* **67,** 145 (1981).
5. Basetto, L., Vaccari, A., and Martini, G., *J. Phys. Chem.* **85,** 1927 (1981).
6. Chianelli, R. R., Prestridge, E. B., Pecoraro, T. A., and de Neufville, J. P., *Science* **203,** 1105 (1979).
7. We wish to thank Dr. T. R. Halbert of this laboratory for the preparation of this sample.
8. Stiefel, E. I., Eisenberger, R., Rosenberg, R. C., and Gray, H. B., *J. Amer. Chem. Soc.* **88,** 2956 (1966).
9. Tauster, S. J., Pecoraro, T. A., and Chianelli, R. R., *J. Catal.* **63,** 515 (1980).
10. According to the method of Eggersten, F. T., and Roberts, R. M., *J. Phys. Chem.* **63,** 1981 (1959). We wish to thank Dr. A. J. Jacobson of this laboratory for the preparation of these samples.
11. Abdo, S., Clarkson, R. B., and Hall, W. K., *J. Phys. Chem.* **80,** 2431 (1976).
12. Johnston, D. C., Jacobson, A. J., Silbernagel, B. G., Frysinger, S. P., Rich, S. M., and Gehbard, L. A., *Solid State Commun.,* in press.
13. One of a series of samples prepared by F. J. Parker and A. F. Ruppert. A detailed report will appear elsewhere.
14. Silbernagel, B. G., *J. Catal.* **56,** 315 (1979).
15. Voorhoeve, R. J. H., and Wolters, H. B. M., *Z. Anorg. Allg. Chem.* **376,** 165 (1970).
16. Abdo, S., La Jacono, M., Clarkson, R. B., and Hall, W. K., *J. Catal.* **36,** 330 (1975).
17. Radhakrishna, S. E., Chowdari, B. V. R., and Viswanath, A. K., *J. Chem. Phys.* **66,** 2009 (1977).
18. Stiefel, E. I., *Prog. Inorg. Chem.* **22,** 1 (1977).
19. Gazzinelli, R., and Schirmer, O. F., *J. Phys. C* **10,** L145 (1977).